

RESEARCH ARTICLE

HPV-CCDC106 integration promotes cervical cancer progression by facilitating the high expression of CCDC106 after HPV E6 splicing

Wenhua Zhi^{1,2} | Ye Wei^{1,2} | Cordelle Lazare^{1,2} | Yifan Meng^{1,2} | Ping Wu^{1,2} |
Peipei Gao^{1,2} | Shitong Lin^{1,2} | Ting Peng^{1,2} | Tian Chu^{1,2} | Binghan Liu^{1,2} |
Wencheng Ding^{1,2} | Canhui Cao^{1,2,3}  | Peng Wu^{1,2}

¹Cancer Biology Research Center (Key Laboratory of the Ministry of Education), Tongji Hospital, Tongji Medical College, Huazhong University of Science and Technology, Wuhan, China

²Department of Gynecologic Oncology, Tongji Hospital, Tongji Medical College, Huazhong University of Science and Technology, Wuhan, China

³Department of Obstetrics and Gynecology, Center for Reproductive Medicine, Peking University Shenzhen Hospital, Shenzhen Peking University-The Hong Kong University of Science and Technology Medical Center, Guangdong, China

Correspondence

Peng Wu and Canhui Cao, Cancer Biology Research Center (Key Laboratory of the Ministry of Education), Tongji Hospital, Tongji Medical College, Huazhong University of Science and Technology, Wuhan, China.
Email: pengwu8626@tjh.tjmu.edu.cn and canhuicao@foxmail.com

Funding information

National Natural Science Foundation of China; China Postdoctoral Science Foundation; Shenzhen Science and Technology Innovation Committee; National Key R&D Program of China

Abstract

Human papillomavirus (HPV) integration and high expression of HPV oncogenes (E6 and E7) are important mechanisms for HPV carcinogenesis in cervical cancer. However, the relationship between HPV integration and HPV E6 spliced transcripts, as well as the underlying mechanisms of HPV integration in carcinogenesis after HPV E6 splicing remains unclear. We analyzed HPV-coiled-coil domain containing 106 (CCDC106) integration samples to characterize the roles of HPV integration, E6 spliceosome I (E6*1), and high CCDC106 expression in cervical carcinogenesis. We found that E6 was alternatively spliced into the E6*1 transcript in HPV-CCDC106 integration samples with low p53 expression, in contrast to the role of E6*1 in preventing p53 degradation in cervical cancer cells. In addition, CCDC106 was highly expressed after HPV-CCDC106 integration, and interacted with p53, resulting in p53 degradation and cervical cancer cell progression in vitro and in vivo. Importantly, when E6*1 was highly expressed in cervical cancer cells, overexpression of CCDC106 independently degraded p53 and promoted cervical cancer cell progression. In this study, we explored the underlying mechanisms of HPV-CCDC106 integration in HPV carcinogenesis after HPV E6 splicing, which should provide insight into host genome dysregulation in cervical carcinogenesis.

KEYWORDS

CCDC106, cervical cancer, E6*1, HPV integration

Abbreviations: CCDC106, coiled-coil domain containing 106; cDNA, complementary DNA; CHX, cycloheximide; Co-IP, co-immunoprecipitation; DMEM, Dulbecco's modified eagle medium; E6AP, E3 ubiquitin ligase E6-associated protein; E6*1, E6 spliced transcripts; EdU, 5-Ethynyl-2'-deoxy uridine; FBS, fetal bovine serum; GAPDH: glyceraldehyde-3-phosphate dehydrogenase; Hi-C, high-throughput chromosome conformation capture; HPV, human papillomavirus; IHC, immunohistochemistry; Ncepi, normal cervical epithelial cells; PEG3, paternally expressed 3; 3D, three-dimensional.

This is an open access article under the terms of the Creative Commons Attribution-NonCommercial License, which permits use, distribution and reproduction in any medium, provided the original work is properly cited and is not used for commercial purposes.

© 2022 The Authors. *Journal of Medical Virology* published by Wiley Periodicals LLC.

1 | INTRODUCTION

The incidence of cervical cancer ranks fourth among female malignancies.¹ In 2020, there were 604 000 new cases and 342 000 deaths worldwide.² Persistent high-risk human papillomavirus (HPV) infection is necessary for the development of cervical cancer.³ The E6 and E7 oncoproteins expressed by high-risk HPV are the important causes of cervical cancer,⁴ and integration of HPV into the host genome is a critical event in its carcinogenesis.^{5,6} However, the relationships and roles of HPV integration and oncogene (*E6* and *E7*) spliced transcripts in carcinogenesis remain unclear.

HPV integration is an important event in HPV carcinogenesis and cervical cancer development,^{7,8} and can lead to genome instability, structural rearrangement, and copy number variation.^{9–11} HPV integration also results in changes in host gene expression, for example, loss of tumor suppressor gene function and increase in oncogene expression, which are carcinogenic mechanisms.^{7,12} In this study, we explored the mechanism underlying low p53 expression level after the HPV was integrated into coiled-coil domain containing 106 (*CCDC106*) (HPV-*CCDC106* integration) in cervical cancer from the perspective of HPV integration.

The E6 oncoprotein promotes the malignant transformation of cervical epithelial cells via multiple oncogenic pathways. The E6 oncoprotein forms a complex with E3 ubiquitin ligase E6-associated protein (E6AP) and p53 to degrade p53.^{13,14} However, the E6 oncogene can be transcribed into multiple transcripts through alternative splicing.^{15,16} The E6 spliceosome (E6*), such as the relatively well-studied E6 spliceosome I (E6*_I),¹⁷ are translated into truncated E6 proteins.^{18,19} Although studies have found that truncated E6 protein and complete E6 protein have homologous amino acid sequences²⁰ and high E6* expression, especially E6*_I, is universal in cervical cancer,¹⁷ the role of E6*_I in p53 degradation and whether HPV causes p53 degradation through other mechanisms is unclear.

We previously identified an HPV integration hot spot gene (*CCDC106*) and found increased expression of *CCDC106* after HPV integrated into *CCDC106*.²¹ In cervical cancer, the HPV-*CCDC106* integration changes the three-dimensional (3D) structure of the genome, hijacks the enhancer of *PEG3*, resulting in the upregulation of *CCDC106* oncogene.^{21,22} However, the role of high expression of *CCDC106* in HPV-*CCDC106* integration cervical cancer remains unclear.

In this study, we analyzed HPV-*CCDC106* integration samples to characterize the roles of such integration in cervical cancer. In HPV-*CCDC106* cervical carcinoma with high *CCDC106* expression, the HPV *E6* gene was transcribed into E6*_I, and p53 expression was low. Thus, we further explored the role of HPV-*CCDC106* in HPV carcinogenesis after HPV *E6* mRNA splicing.

2 | METHODS

2.1 | Cell culture and transfection

Human cervical cancer cell lines SiHa (ATCC, HTB-35), HeLa (ATCC, CCL-2), Caski (ATCC, CRL-1550), and HaCaT (CCTCC, GDC0106) were

cultured in Dulbecco's modified eagle medium (DMEM) supplemented with 10% fetal bovine serum (FBS), 100 U/ml penicillin and 100 g/ml streptomycin. The E6*_I with Flag-tag plasmid transfected the cells with X-tremeGENE HP (Roche; 739406). The lentivirus vector Lv-*CCDC106* with DDDDK-tag (GeneChem) was designed to overexpress the level of *CCDC106* stably in SiHa and HeLa cells, and Lv-control was the control lentivirus. The sh*CCDC106* (RIBOBIO) transfected the cells with Lipofectamin3000 Reagent (Thermo Fisher Scientific; L3000015) to disturb the expression of *CCDC106* and the negative control is shNC. The sh*CCDC106* sequences were as follows:

forward 5'-GUCGGAGGCGGACAAUGAATT-3',
reverse 5'-UUCAUUGUCCGCCUCGACTG-3'.

2.2 | Western blot assay

Collect the cells and lyse the cells by RIPA (Servicebio; G2002) supplemented with a protease inhibitor cocktail (Servicebio; G2006). Thirty micrograms of total protein samples were separated by 10% sodium dodecyl sulfate-polyacrylamide gel electrophoresis and proteins were transferred onto the polyvinylidene fluoride (PVDF) membrane. The primary antibodies glyceraldehyde-3-phosphate dehydrogenase (GAPDH) (1:10000, AC002), p21 (1:1000, A2691), CyclinB1 (1:1000, A2056), Gadd45a (1:1000, A11768) were obtained from ABclonal, p53 (1:1000; Proteintech; 13244-1-AP), E6 (1:1000; Santa Cruz Biotechnology; sc-460), Flag-Tag Antibody (1:1000; AE005; ABclonal), and *CCDC106* (1:1000; ab105354) were used. The membrane was blocked with 5% BSA and incubated with primary antibodies for 12 h at 4°C. A corresponding second antibody (1:5000; antGENE; ANT020; ANT19) was used to incubate the membrane for 1 h and then exposed to the PVDF membrane by enhanced chemiluminescence solution.

2.3 | Immunofluorescence

Cells were seeded on the slide, fixed with paraformaldehyde and permeabilized with 0.5% Triton X-100. Cells were incubated overnight at 4°C with primary antibodies:p53 (1:50; Proteintech; 13244-1-AP), E-cadherin (1:100; GeneTex; GTX100443), and Flag-Tag Antibody (1:50; AE005; ABclonal) incubation with corresponding secondary fluorescent antibody (1:200; Cy3 Anti-Mouse IgG; AS008; and FITC Anti-Rabbit IgG AS011; ABclonal). 4',6-Diamidino-2'-phenylindole stained nucleus. Observed cells and took pictures under a fluorescence microscope.

2.4 | Immunoprecipitation assay

SiHa cells were transfected with Lv-*CCDC106* with the DDDDK-tag. The cell lysates were prepared by IP Kit (Thermo Fisher Scientific; 26147) and incubated lysates with DDDDK-tag magnetic beads (Bimake; B26101) at 4°C overnight. Protein was eluted from the beads and analyzed by Western blot analysis.

2.5 | Real-time PCR

Extract total RNA from cells by RNAiso Plus (Takara; 9109), and reverse transcript total RNA into complementary DNAs by Reverse transcription kit HI Script III qRT Super Mix (Vazyme; R323-01). And every real-time PCR reaction system contains 10 μ l SYBR Green Real-time PCR Mix (Vazyme; Q141-02) and the program is as follows: 95°C for 3 min and 40 cycles of 95°C for 10 s, 60°C for 30 s, and 95°C for 15 s. GAPDH and EEF1A1 were internal references. The primers were in Supporting Information: Table 1.

2.6 | Immunohistochemistry

Four micrometers of tissue slices were sliced from paraffin-embedded specimens. All the paraffin-embedded specimens came from the pathology department of Gynecology of Tongji Hospital and pathologic diagnosis was confirmed by at least two experienced pathological diagnosis physicians. The primary antibodies were used: p53 (1:300; MBL; K0181-03); CCDC106 (1:200; Gene Tex; GTX27918), Ki67 (1:500; Servicebio; GB111499). The corresponding HRP-conjugated secondary antibodies (ZSGB-BIO; SP-9001; SP-9002) were incubated for 30 min at room temperature. Colorimetric detection was detected by a DAB staining kit (1:100; Servicebio; G1212-200T). The scoring method was as follows: percentage of cells stained was scored as 0 (<5%), 1 (5%–25%), 2 (26%–50%), and 3 (51%–75%), and 4 (76%–100%); staining intensity was scored as 0 (colorless), 1 (light yellow), 2 (brownish yellow), and 3 (brown). Both scores per slide were multiplied as a final score :0 representing negative expression (-), while scores 1–4, 5–8, and 9–12 represented weak positivity (+), positive (++), and strong positivity (+++).

2.7 | Transwell assay

8×10^4 SiHa cells or 4×10^4 HeLa cells resuspended with 100 μ l serum-free DMEM were seeded in the upper chamber and DMEM with 20% FBS was added into the basolateral chamber for 12 h. The apical chamber was fixed with paraformaldehyde and dyed with crystal violet. The cell number was counted under a microscope and choose 3–5 fields for counting in each group.

2.8 | Scratch assay and colony formation assay

Cells were seeded in the well plate and scratched with a 200 μ l pipette tip, and then cultured the cells in DMEM supplemented with 2% FBS for 24–48h. Measure the distance of the scratch wound by ImageJ software. One thousand were seeded into well plates and cultured for 2 weeks. Cells were fixed with formaldehyde and stained with crystal violet, then scanned under a scanner, and the cell colonies were measured randomly under an inverted microscope.

2.9 | CCK8 assay

Four thousand cells were seeded into 96-well plates. Cell Counting Kit-8 (Dojindo; CK04) was used to measure cell viability according to the manufacturer's instructions. Measured the cell viability once a day for 4 consecutive days under 450 nm using an automated microplate reader (SpectraMax190; Molecular Devices) and draw a cell activity curve.

2.10 | Flow cytometry for cell cycle analysis

Cells transfected with shRNA or lentiviral vector were fixed in 70% anhydrous ethanol for 4–6 h and then stained with propidium iodide and RNase A for 30 min at room temperature. Data were collected using BD systems and analyzed by FlowJo VX10.

2.11 | GST pull-down assay

We constructed CCDC106 prokaryotic expression vector with a GST label and the TP53 expression vector with HIS label by WZ Biosciences. IPTG (Solarbio; #I8070-1g) induced the expression of GST-CCDC106 or HIS-TP53. Total bacterial protein was extracted and GST-CCDC106 and HIS-TP53 proteins were purified with a purification kit (Abbkine; KTP2001; KTP2010). GST pull-down assay was performed according to kit steps (DianAn Biotechnology; K0077). Proteins were isolated by Western blot.

2.12 | 5-Ethynyl-2'- deoxy uridine assay

Cell-Light 5-Ethynyl-2'- deoxy uridine (EdU) Apollo567 In Vitro Kit (100 T) (RIBOBIO; C10310-1) was used for the EdU assay. EdU replaces thymine (T) during DNA replication. DNA replication activity can be detected based on the specific reaction of Apollo® fluorescent Dye and EdU. Hoechst tags living cells. After the kit procedure was followed, photos were taken under the fluorescence microscope. After the kit procedure was followed, photos were taken under the fluorescence microscope (BX53; Olympus).

2.13 | Mouse subcutaneous xenograft tumor model

BALB/c nude mice (female, 6–8 weeks old) were housed in the Laboratory Animal Management Center of Tongji Hospital. Cells transfected in Lv-control, Lv-CCDC106, or E6*1 were prepared as $1 \times 10^7/100 \mu$ l, and 1×10^7 transfected cells were injected subcutaneously into the armpit of nude mice. Every group has five nude mice for repeat and parallel.

2.14 | Bioinformatic analysis

Hi-C data of samples, including cervical cancer (Carcinoma*) and Ncepi, were downloaded from the Genome Sequence Archived data set (GSA; CRA001401; <http://bigd.big.ac.cn/gsa/>). A/B Compartment analysis was performed as the previous study.²¹ A/B Compartment of chromosome 19 (GRCh37/hg19) was analyzed to show the expression status of HPV integration regions. Single-cell sequencing data of the normal cervix was downloaded from Human Cell Landscape (HCL) (<https://db.cngb.org/HCL/>).⁴⁵ The CCDC106 expression feature plot of the normal cervix was performed according to the CCDC106 expression intensity of each cell, cells were clustered into 12 clusters.

2.15 | Statistical analysis

The data are presented as the mean \pm SD acquired from at least three independent experiments. Prism 6.0 GraphPad Software was used to perform statistical analyses. Comparisons between two groups were done by Student's *t*-test. Correlation analyses were done using the Spearman rank test. **p* < 0.05, ***p* < 0.01, and ****p* < 0.001 were considered statistically significant.

3 | RESULTS

3.1 | HPV16 E6 was spliced into E6*1 and CCDC106 was highly expressed with the low p53 expression in HPV-CCDC106 integration cervical carcinomas

We previously identified the 3D structure of the HPV16-CCDC106 integration sample (Carcinoma*) via high-throughput chromosome conformation capture (Hi-C).²¹ In the current study, we reanalyzed the Carcinoma* samples, with normal cervical epithelial cells (Ncepi) used as the control (Figure 1A). Based on Hi-C analysis, the A/B compartments of the HPV-CCDC106 integration site changed from the A to B compartment, indicating that HPV integration changed the chromosome status (Figure 1B). Ten HPV-CCDC106 integration samples²¹ were collected to demonstrate the higher CCDC106 expression in HPV-CCDC106 samples compared with normal cervix samples by real-time PCR (Figure 1C). Through analysis of the RNA-sequencing (RNA-seq) data of the HPV-CCDC106 integration Carcinoma* and Ncepi sample, the HPV16 E6 oncogene was found to be expressed in the E6* form, lacking 226–409 bp of the full-length E6 transcript (Figure 1D). This spliceosome transcript was therefore identified as the sequence of E6*1,²³ and was ubiquitously expressed in the HPV-CCDC106 integration samples (Figure 1E and Supporting Information: Figure S1A). Although E6 is believed to be the reason for p53 degradation in cervical cancer,¹³ the role of E6*1 in p53 degradation remains controversial. Here, we analyzed the p53 level of 10 HPV-CCDC106 integration samples and 10 samples without HPV-CCDC106 integration, and 12 normal cervix samples. Immunohistochemistry (IHC) analysis showed that the expression of p53

was low in the HPV-CCDC106 integration samples compared with the normal cervix and samples without HPV-CCDC106 integration (Figure 1F and Supporting Information: Figure S1B), and western blot analysis showed that p53 protein expression was low in the Carcinoma* (Figure 1G). To investigate other potential pathways for p53 degradation, we analyzed the expression levels of genes related to p53 degradation in the Carcinoma* HPV-CCDC106 sample via RNA-seq. Compared with the Ncepi sample, the expression levels of p53 degradation-related genes were lower and CCDC106 mRNA levels were higher in the Carcinoma* sample (Figure 1H). In addition, single-cell sequencing data analysis showed that CCDC106 expression levels in the normal cervix sample were universally low (Figure 1I). RNA-seq analysis from Gene Expression Profiling Interactive Analysis and Gene Expression Omnibus database data sets showed that the expression levels of CCDC106 were moderate in cervical cancer compared with the other cancer types (Supporting Information: Figure S2A–B). Lv-CCDC106 vector could significantly up-regulate CCDC106 expression in SiHa and HeLa cells (Supporting Information: Figure S2C).

3.2 | Overexpression of E6*1 suppressed tumor progression by inhibiting p53 degradation in cervical cancer cells

We investigated the biological roles of E6*1 in SiHa cervical cancer cells, which do not express E6*1 (Supporting Information: Figure S3A). After transfection of E6*1 plasmids into the SiHa cells, both cell proliferation and migration were inhibited (Figure 2A–C). At the same time, the expression levels of p53 and E-cadherin in SiHa-E6*1 cells increased (Figure 2D,E). These results indicated that E6*1 may inhibit cell proliferation and migration by upregulating p53 and E-cadherin levels. After inhibiting the synthesis of total cell protein with cycloheximide (CHX), the p53 degradation rate in the SiHa-E6*1 cells was significantly lower than that in the control group (Figure 2F). After subcutaneous implantation of SiHa control and SiHa-E6*1 cells into nude mice, compared with the SiHa control, the SiHa-E6*1 tumors showed smaller volume and weight (Figure 2G,H) and a lower Ki67-positive rate by IHC (Figure 2I and Supporting Information: Figure S3B). These results indicated the negative effects of E6*1 on tumor growth. Thus, unlike the E6 oncoprotein, E6*1 appeared to prevent rather than promote p53 degradation. After transfection of E6*1 into HaCaT cells, we found that E6*1 could not degrade p53 (Supporting Information: Figure S3C), and there was no difference between the over-E6*1 expressed group and the control group in the cell proliferation of Cell Counting Kit-8 (CCK8) and EdU assays (Supporting Information: Figure S3D and S3E).

3.3 | Overexpression of CCDC106 promoted p53 degradation by p53 interaction

As E6*1 did not promote p53 degradation, we further explored the potential mechanism underlying p53 degradation in the HPV-CCDC106

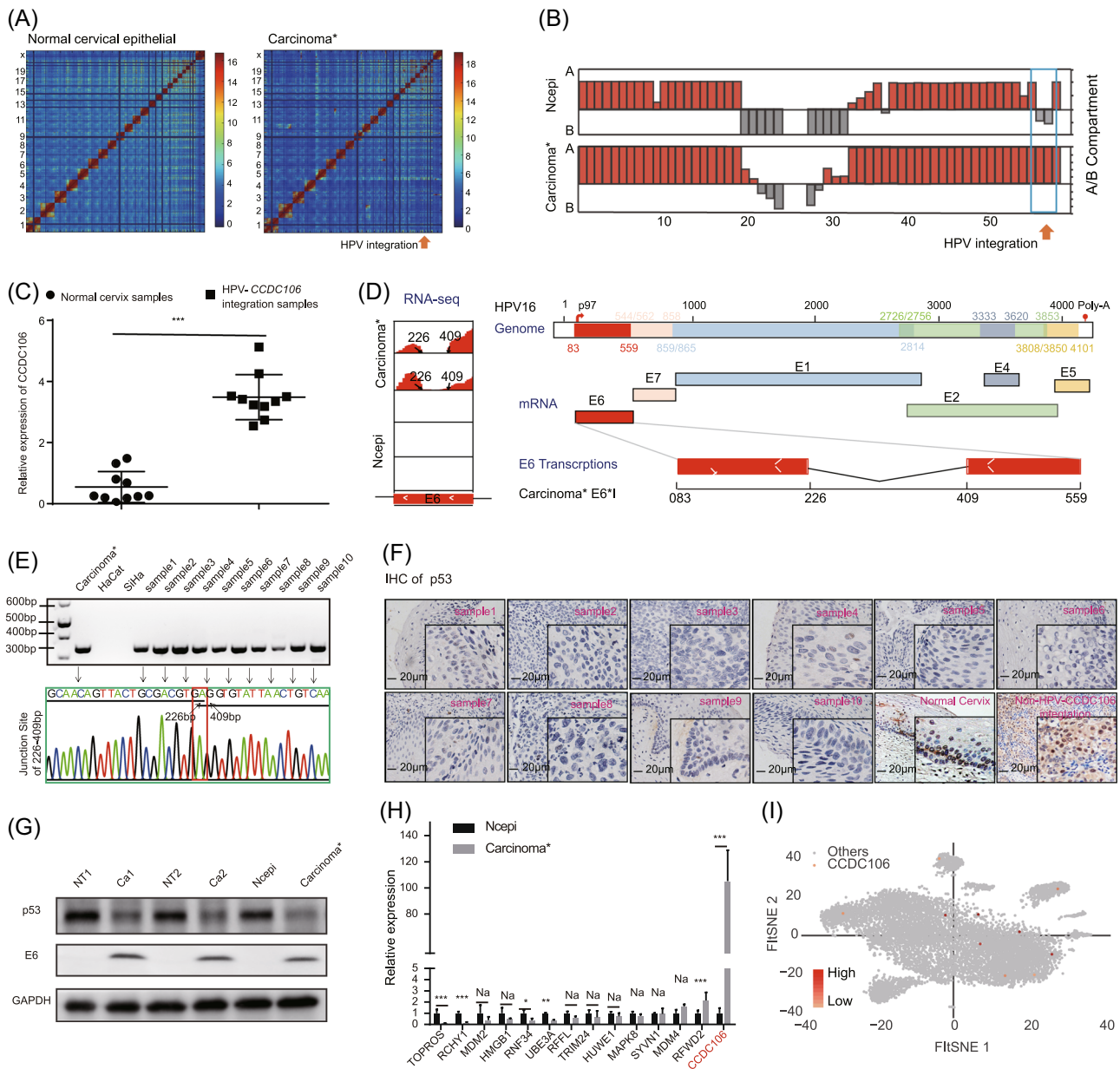


FIGURE 1 *E6*1* and *CCDC106* were highly expressed with low p53 expression in HPV-*CCDC106* integration samples. (A) Heatmaps of the whole genome of normal cervical epithelia and Carcinoma*. Arrow indicated the HPV integration locus. (B) A/B compartment of *CCDC106* changed from A compartment to B compartment in a blue box. (C) Relative mRNA expression of *CCDC106* in normal cervix samples and HPV-*CCDC106* samples by real-time-PCR ($n = 10$). (D) RNA sequence of *E6* is missing 226-409 bp in the Carcinoma* and the Ncepi sample has no *E6* RNA sequence. Sequence diagram of *E6*1* spliced from *E6*. (E) Agarose gel electrophoresis of the *E6*1* cDNA obtained in HPV-*CCDC106* integration samples and the SiHa and Ha Cat cell line. And the 226-409 bp junction site of *E6*1* was circled by a red frame. (F) IHC staining of p53 in the HPV-*CCDC106* integration samples, and the representative picture of p53 staining in normal cervix and sample without HPV-*CCDC106* integration. (G) The p53 and E6 levels of the Carcinoma* sample compared with cervical cancer and no carcinoma tissues by Western blot. GAPDH was an internal reference. (H) The relative RNA level of genes related to p53 degradation in Carcinoma* and Ncepi by RNA-seq. (I) The expression level of *CCDC106* in normal cervix sample by single-cell sequencing. Ca, cervical carcinoma tissue; cDNA, complementary DNA; *E6*1*, *E6* spliced transcripts; GAPDH, glyceraldehyde-3-phosphate dehydrogenase; HPV, human papillomavirus; IHC, immunohistochemistry; Na, negative significance; Ncepi, normal cervical epithelial cells; NT, no carcinoma tissues; RNA-seq, RNA-sequencing.

integration samples, focusing on high *CCDC106* expression. Here, sh*CCDC106* was used to disturb the expression of *CCDC106* and the lentiviral vector Lv-*CCDC106* was used to increase the exogenous expression of *CCDC106* in the SiHa and HeLa cell lines (Figure 3A and

Supporting Information: Figure S4A). The RNA levels of *E6* and *E6*1* were not affected by changes in *CCDC106* expression in the SiHa and HeLa cells (Figure 3B). Western blot analysis showed that high expression of *CCDC106* reduced the level of p53 in SiHa and HeLa

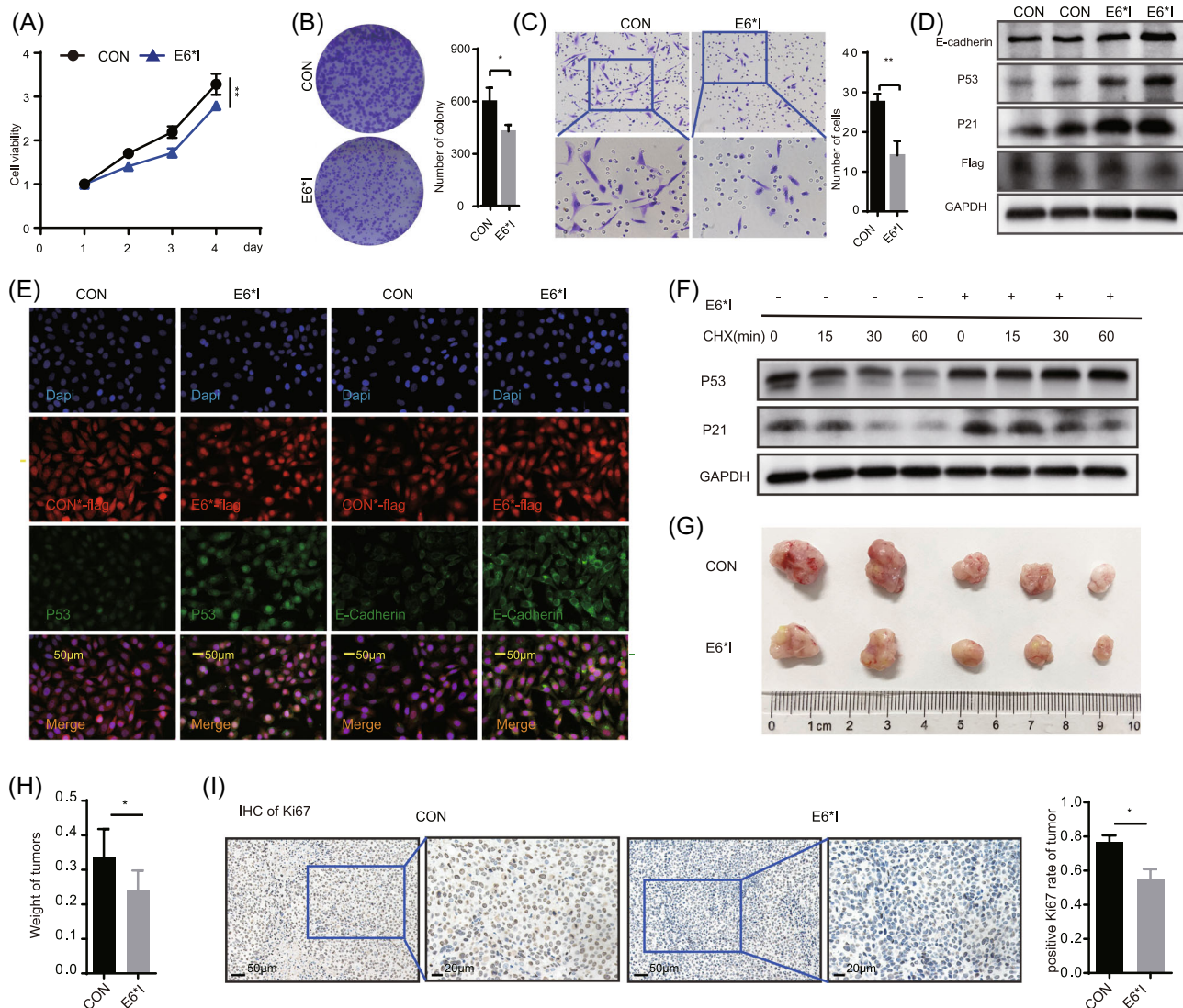


FIGURE 2 E6*1 suppressed the tumor progression by inhibiting p53 degradation. (A–C) Cell proliferation by CCK8 assay (A), colony formation assay (B), and the cells spreading by transwell assay (C) after transfected E6*1 plasmid in SiHa cells ($n = 3$). (D, E) p53, p21, Flag, and E-cadherin expression in the SiHa control and SiHa-E6*1 cells by Immunofluorescence and Western blot. The E6*1-flag protein represents the expression of the E6*1 plasmid with a Flag tag. (F) Expression of p53 and p21 by Western blot after treatment with 50 nmol/ml CHX for 15, 30, 60 min in SiHa transfected in E6*1 plasmid and control. (G) Subcutaneous tumor burdens of SiHa-E6*1 cell and control ($n = 5$ per group). (H) Comparison of tumor weight between SiHa-E6*1 tumors and control ($n = 5$). (I) The representative images and comparisons of Ki67 immunohistochemical staining of subcutaneous tumor ($n = 5$). GAPDH was the internal reference. CCK8, Cell Counting Kit-8; CHX, cycloheximide; E6*1, E6 spliced transcripts; GAPDH, glyceraldehyde-3-phosphate dehydrogenase.

cells, whereas the p53 expression increased after disturbing the expression of CCDC106. Moreover, the expression of downstream proteins, such as p21, cyclinB1, and Gadd45a, also changed with p53 expression, especially the cell cycle-regulated protein p21 (Figure 3C,D). High expression of CCDC106 in HaCaT cells also reduced the level of p53 (Supporting Information: Figure S4B). We collected 50 cervical cancer specimens from a clinical center for immunohistochemical analysis. The clinical information of the patient samples was in the Supporting Information: Table 2. Results showed a negative correlation between the expression of CCDC106 and p53 after immunoreactive score analysis (Figure 3E). We also performed an immunoprecipitation assay (Figure 3F) and GST pull-down assay (Supporting Information:

Figure S4C), which showed that CCDC106 interacted with the p53 protein. Thus, these results indicated that CCDC106 degraded p53 expression via interaction with p53 and high CCDC106 expression promoted p53 degradation in HPV-CCDC106 samples.

3.4 | Overexpression of CCDC106 promoted proliferation and migration of cervical cancer cells

To further investigate its biological functions, we explored the role of CCDC106 in the migration of cervical cancer cells using scratch and transwell assays. We observed that the speed of wound healing

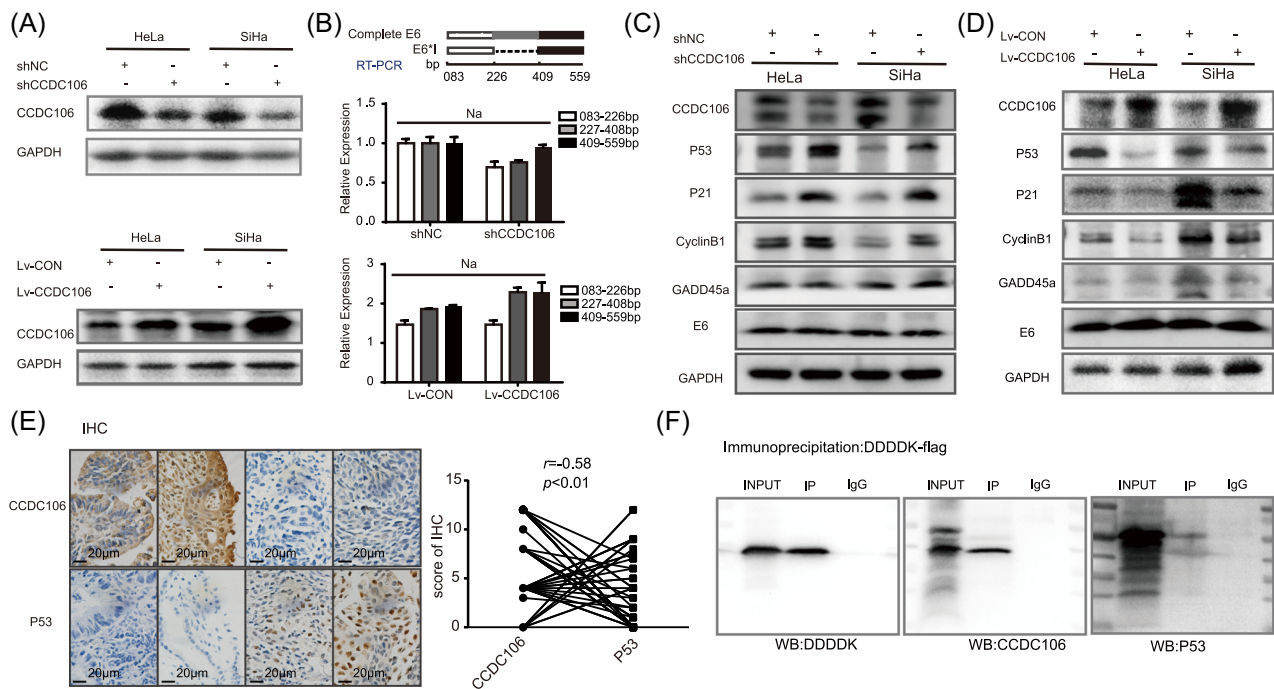


FIGURE 3 Overexpression of CCDC106 promoted p53 degradation by interacting with p53. (A) The protein expression level of CCDC106 after interference or overexpression of CCDC106 by shCCDC106 and Lv-CCDC106 in SiHa and HeLa cells. (B) The three fragments of E6 mRNA level after transfected shRNA and Lv-CCDC106 in SiHa cells. White bar: 063–226 bp fragment, gray bar: 226–409 bp fragment, black bar: 409–559bp fragment ($n = 3$). (C, D) E6, p53, p21, cyclinB1, and Gadd45a proteins were analyzed by Western blot after interference or overexpression of CCDC106. (E) Representative images of CCDC106 and p53 in cervical cancer samples by immunohistochemistry. Spearman rank test analyzed the correlation between the expression level of CCDC106 and p53 ($n = 50$). r and p Values were analyzed by the Spearman rank test. (F) Lv-CCDC106 with DDDDK tag was transfected into SiHa. Immunoprecipitation was performed by DDDDK magnetic beads. DDDDK, p53, and CCDC106 were analyzed by Western blot. GAPDH was the internal reference. GAPDH, glyceraldehyde-3-phosphate dehydrogenase; Na, negative.

and the number of escaped cells were higher in CCDC106-overexpressed cells, indicating that high CCDC106 expression promoted cervical cancer cell migration (Figure 4A,B, Supporting Information: Figure S5A and S5B). Based on cell viability (CCK8 test) and cell colony number after 2 weeks (colony formation assay), the proliferation of SiHa and HeLa cells was inhibited after shCCDC106 interference on CCDC106 expression, and proliferation of Lv-CCDC106 cells with high CCDC106 expression increased compared with the control (Figure 4C,D and Supporting Information: Figure S5C). In addition, high expression of CCDC106 in HaCaT cells promoted cell proliferation by CCK8 and EdU test (Supporting Information: Figure S5D and S5E). Cell flow cytometry showed that the percentage of S-stage cells increased in the high CCDC106-expressing cells (Figure 4E). After subcutaneous implantation of SiHa control and SiHa-Lv-CCDC106 cells into nude mice, the volume and weight of the SiHa-Lv-CCDC106 tumors were higher than that of the control (Figure 4F), and the Lv-CCDC106 expressing tumors had a higher Ki67-positive rate (Figure 4G and Supporting Information: Figure S5F). These results demonstrate that high CCDC106 expression may promote the proliferation and migration of cervical cancer cells via degradation of p53 in vitro and in vivo.

3.5 | Overexpression of CCDC106 promoted cervical cancer progression and p53 degradation during E6*1 overexpression

Here, high CCDC106 and E6*1 expression played opposite roles in p53 degradation in the cervical cancer cells, and both occurred in the HPV-CCDC106 integration samples. Thus, we next investigated the biological function of high CCDC106 expression with HPV16 E6*1 overexpression. We cotransfected Lv-CCDC106 into SiHa-E6*1 cells to overexpress both CCDC106 and E6*1 in SiHa cells. SiHa-E6*1 inhibited cell wound healing and migration compared with SiHa control, but SiHa-E6*1-Lv-CCDC106 cells overexpressing CCDC106 promoted wound healing and migration by scratch assays and transwell (Figure 5A,B). Furthermore, based on the CCK8 and colony formation assays, SiHa-E6*1 cells overexpressing CCDC106 proliferated faster than SiHa-E6*1 cells (Figure 5C,D and Supporting Information: Figure S6A). The growth of subcutaneous tumors in mice overexpressing CCDC106 and E6*1 was faster than that in the group overexpressing E6*1 alone (Figure 5E and Supporting Information: Figure S6B), and had a higher Ki67-positive rate (Figure 5F and Supporting Information: Figure S6C). Western blot analysis also showed that p53 increased in the SiHa cells expressing E6*1 alone,

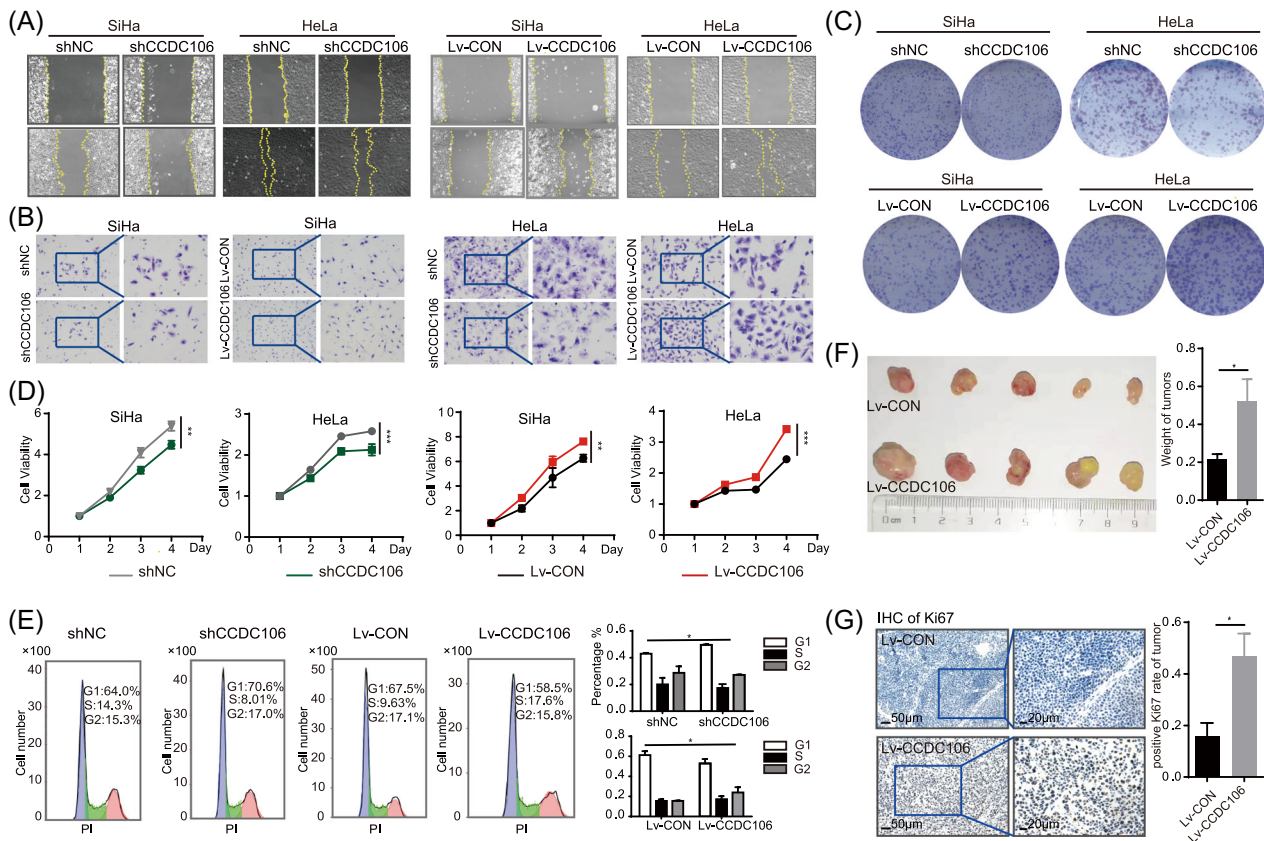


FIGURE 4 Overexpression of CCDC106 promoted proliferation and migration of cervical cancer cells. (A) Migration speed was analyzed by scratch assay after transfected with shCCDC106 and Lv-CCDC106 for 48 h. (B) The spreading ability of SiHa and HeLa after being transfected with shCCDC106 and Lv-CCDC106 by transwell assay. (C) Colony formation of SiHa and HeLa after transfected with shCCDC106 and Lv-CCDC106. (D) Proliferation rate of SiHa and HeLa after transfected with shCCDC106 and Lv-CCDC106 by CCK8 test. (E) Cell cycle distribution percentage between NC, shRNA, Lv-CON, and Lv-CCDC106 groups (n = 3). (F) Subcutaneous tumor burdens and comparison of tumor weight after overexpression of Lv-CCDC106 in SiHa (n = 5 per group). (G) The representative images and comparison of Ki67 immunohistochemical staining of subcutaneous tumor. The black bar is SiHa-Lv-control, and the gray bar is SiHa-Lv-CCDC106 (n = 5). CCK8, Cell Counting Kit-8.

but high expression of CCDC106 reduced the level of p53 in SiHa-E6*1 cells (Figure 5G). CCDC106 promoted p53 degradation by binding to p53 and facilitating its ubiquitination.²⁴ Proteasome inhibitor MG132 was used for inhibiting the ubiquitin-proteasome degradation pathway for 12 h, the p53 levels were not changed by overexpression of CCDC106 in SiHa-E6*1 cells (Figure 5H). The p53 degradation in SiHa-E6*1 cells overexpressing CCDC106 was faster than that in SiHa-E6*1 cells after treatment with CHX (Figure 5I). Under E6*1 overexpression, high CCDC106 expression promoted the proliferation and migration of cervical cancer and degraded p53 independently.

4 | DISCUSSION

In this study, we found that E6*1 not only failed to degrade the tumor suppressor protein p53 but prevented its degradation in SiHa. However, high CCDC106 expression caused by HPV-CCDC106 integration could degrade p53 by directly binding to p53 and promote the malignant progression of tumors in vivo and in vitro, opposite to the role of E6*1 on p53.

HPV integration may change critical cellular genes, leading to loss of tumor suppressor gene function, enhanced expression of oncogenes, loss of DNA repair gene function, and other cell function changes.²⁵ The expression of HPV integration site genes is significantly higher than the expression level of the same genes in unintegrated sites. For example, HPV integration near the MYC gene leads to excessive MYC rearrangement and overexpression.¹⁰ HPV integration results in a significant upregulation in the transcription activity of the proximal genome elements, including the transcription of genomic elements not normally expressed.²⁶ In addition, the transcriptional activity of flanking cellular sequences increases near HPV integration sites²⁷ and HPV integration is highly related to transcriptional activity in the host genome integration region.²⁸ Studies have found that HPV integration produces a super-enhancer-like element consisting of a tandem copy of the upstream regulatory region of the virus and a cellular enhancer to drive high expression of viral oncogenes and nearby human genes.²⁷

CCDC106 is a hot site for HPV integration, and the expression level and 3D structure of CCDC106 changes following HPV integration, as reported in our earlier study.²¹ In this research, the

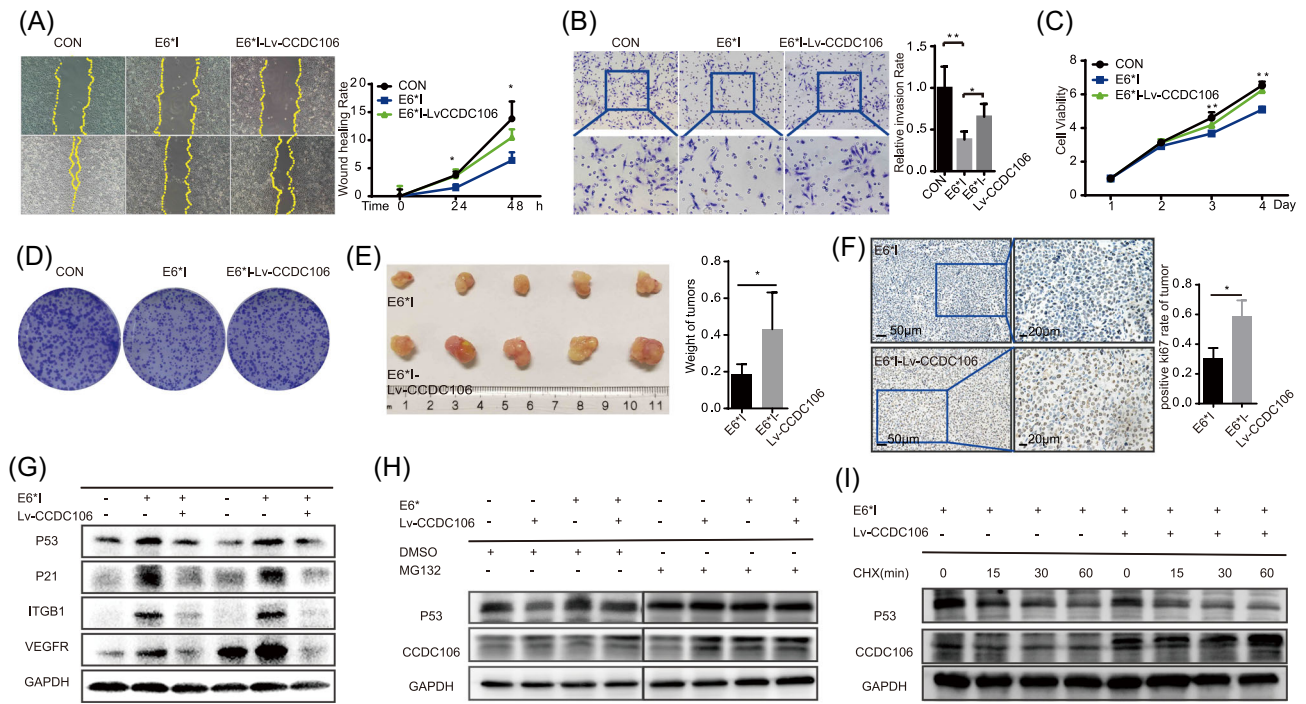


FIGURE 5 Overexpression of CCDC106 promoted cervical cancer progression and p53 degradation during E6*1 overexpression. (A, B) Comparison of migration speed between SiHa-E6*1 cells and SiHa-E6*1-LvCCDC106 cells and Control cells by scratch assay and transwell assay ($n=3$). (C, D) Cell proliferation was analyzed by CCK8 assay and colony formation assay was performed after transfecting the Lv-CCDC106 in SiHa-E6*1 cells ($n=3$). (E) Subcutaneous tumor burdens of tumor weight after overexpression Lv-CCDC106 in SiHa-E6*1 ($n=5$). (F) The representative images and comparisons of Ki67 immunohistochemical staining in subcutaneous tumor ($n=5$ per group). (G) CCDC106, p53, p21, E-cadherin, E6, and ITGB1 expression in coexpression of E6*1 and Lv-CCDC106 cells. (H) Western blot was performed to analyze the p53 after the treatment of 2 $\mu\text{mol/ml}$ MG132 for 12 h. (I) Analysis of p53 and CCDC106 by Western blot after treatment SiHa-E6*1 and SiHa-E6*1-Lv-CCDC106 cells with 50 nmol/ml CHX for 15, 30, 60 min. GAPDH was the internal reference. CCK8, Cell Counting Kit-8; CHX, cycloheximide; E6*1, E6 spliced transcripts; GAPDH, glyceraldehyde-3-phosphate dehydrogenase.

integration of HPV into *CCDC106* promoted the expression of *CCDC106*, in turn, degraded p53 and promoted malignant tumor progression. Therefore, degradation of p53 is not only caused by the E6 but also by HPV-*CCDC106* integration.

In the previous research, E6*1 is spliced from the high-risk HPV E6 polycistronic mRNA transcript,¹⁷ and its expression is related to the splicing factors hnRNPA1, hnRNPA2, BRM, and SAM68,²⁹ whereas E6*1 is not detected in low-risk HPV.³⁰ E6*1 is the most abundant E6 spliceosome in cervical cancer by RNA-seq.³¹ E6*1 and complete E6 proteins have homologous amino acid sequences and previous studies explore the expression and function of E6*1 by constructing an exogenous vector of E6*1 with fused tag proteins.^{19,20} Studies have found E6*1 is significantly increased during the progression of cervical cancer,³² and E6 mRNA splicing favors the high expression of the E7 oncogene.³³ In the early stage of HPV carcinogenesis, p53 degradation induced by E6 inhibits cell apoptosis and leads to genomic instability,³⁴ which is an important HPV carcinogenic mechanism, and splicing of E6 transcript and high expression of E7 may be more conducive to the malignant proliferation of cells in the further development of carcinogenesis.^{33,35} Although E6*1 can bind with E6-AP and E6, it cannot degrade p53.^{29,36} Conversely, E6*1 is reported to reverse the p53 degradation

of E6,³⁷ and competitively bind E6-AP with E6 for inhibiting p53 degradation.¹⁷ In this study, we validated that E6*1 could not degrade p53 in HaCaT cells but upregulated p53 expression in SiHa cells, which was consistent with previous studies. E6*1 can also reduce tumor formation of cervical cancer cells in vivo,³⁸ which may be related to its upregulation of p53 expression, as suggested by our data. These results indicate that E6*1 harms cervical cancer tumor growth; however, the biological activity of E6*1 is complex and needs to be further explored.

As an important tumor-related gene, p53 function is abnormal in most human cancers.³⁹ In about half of malignant tumors, mutations in the *TP53* gene directly lead to the inactivation of p53.⁴⁰ The expression level of the p53 protein is mainly determined by its degradation rate, not its production.^{41,42} E3 ligases are an important family to mediate ubiquitin-proteasome degradation pathways and are also important for p53 degradation.⁴¹ Multiple E3 ligases have been reported, among which E6-AP is a HECT-type E3 ligase. High-risk HPV E6 combines with E6-AP to degrade p53 in cervical cancer,¹³ resulting in the low expression of p53 in HPV-positive cervical cancers. In cervical cancer, *TP53* mutations and HPV integration are mutually exclusive.⁴³ In the samples we studied, HPV16 E6 failed to degrade p53 because it was transcribed into E6*1.

Therefore, we considered that HPV may degrade p53 in multiple ways. We also found that the transcriptional activity and expression level of CCDC106 increased following HPV-CCDC106 integration. Previous studies have reported that CCDC106 can bind to p53 to promote its degradation.^{24,44} Thus, important oncogenic pathways, such as p53, are not only regulated by HPV oncogenes in cervical cancer but also by changes in host gene expression caused by HPV integration.

Our study is limited by the small HPV-CCDC106 integration sample size and the lack of E6*1 antibodies. Although previous studies suggest changes in the 3D structure of genes may be involved,²¹ the mechanisms related to the increase in CCDC106 expression following HPV-CCDC106 integration need to be further explored. In addition, the mechanisms of upregulation for integrated genes near the integration site in HPV-related or viral-related carcinoma need to be determined.

5 | CONCLUSIONS

In summary, we found that E6*1 antagonized the complete E6 protein and prevented p53 degradation. We also found that the increase of CCDC106 expression caused by HPV-CCDC106 integration promoted cervical cancer progression by degrading p53, thus highlighting the carcinogenic mechanism underlying HPV integration in cervical cancer. These results indicate that host genome changes caused by HPV integration are partially responsible for cervical cancer progression.

AUTHOR CONTRIBUTIONS

Peng Wu and Canhui Cao conceived this study and made critical revisions to the manuscript. Wenhua Zhi designed this study, drafted the manuscript, and reviewed all references. Ye Wei, Cordelle Lazare, Yifan Meng, Peipei Gao, Ping Wu, Shitong Lin, Ting Peng, Tian Chu, Binghan Liu, and Wencheng Ding aided in study design, samples collection, and data analysis.

ACKNOWLEDGMENT

The results shown here are partly based upon data generated by the Genome Sequence Archived data set and Human Cell Landscape (HCL). This work was supported by the National Key R&D Program of China (2021YFC2701201), the National Natural Science Foundation of China (grant numbers 82072895 and 82141106), China Postdoctoral Science Foundation (2021M702223), and Shenzhen Science, and Technology Innovation Committee (JCYJ20210324105808022, RCBS20210706092345027).

CONFLICT OF INTEREST

The authors declare no conflict of interest.

DATA AVAILABILITY STATEMENT

All data and materials supporting the findings are available from its supplementary information files and from the corresponding author upon reasonable request.

ETHICS STATEMENT

This study was approved by the Ethics Committee of Tongji Medical College of Huazhong University of Science and Technology. For patients: ID ([2020] S224), Date: 2020.09.09. For animals: ID (TJH-202111019), Date: 2021.09.22.

ORCID

Canhui Cao  <http://orcid.org/0000-0002-7328-0264>

REFERENCES

- Sung H, Ferlay J, Siegel RL, et al. Global cancer statistics 2020: GLOBOCAN estimates of incidence and mortality worldwide for 36 cancers in 185 countries. *CA Cancer J Clin.* 2021;71(3):209-249. doi:10.3322/caac.21660
- Bray F, Ferlay J, Soerjomataram I, Siegel RL, Torre LA, Jemal A. Global cancer statistics 2018: GLOBOCAN estimates of incidence and mortality worldwide for 36 cancers in 185 countries. *CA Cancer J Clin.* 2018;68(6):394-424. doi:10.3322/caac.21492
- Walboomers JM, Jacobs MV, Manos MM, et al. Human papillomavirus is a necessary cause of invasive cervical cancer worldwide. *J Pathol.* 1999;189(1):12-19. doi:10.1002/(sici)1096-9896(199909)189:1<12::aid-path431>3.0.co;2-f
- Spurgeon ME, den Boon JA, Horswill M, et al. Human papillomavirus oncogenes reprogram the cervical cancer microenvironment independently of and synergistically with estrogen. *Proc Natl Acad Sci USA.* 2017;114(43):E9076-E9085. doi:10.1073/pnas.1712018114
- Hu Z, Zhu D, Wang W, et al. Genome-wide profiling of HPV integration in cervical cancer identifies clustered genomic hot spots and a potential microhomology-mediated integration mechanism. *Nat Genet.* 2015;47(2):158-163. doi:10.1038/ng.3178
- Integrated genomic and molecular characterization of cervical cancer. *Nature.* 2017;543(7645):378-384. doi:10.1038/nature21386
- McBride AA, Warburton A. The role of integration in oncogenic progression of HPV-associated cancers. *PLoS Pathog.* 2017;13(4):e1006211. doi:10.1371/journal.ppat.1006211
- Schmitz M, Driesch C, Jansen L, Runnebaum IB, Durst M. Non-random integration of the HPV genome in cervical cancer. *PLoS One.* 2012;7(6):e39632. doi:10.1371/journal.pone.0039632
- Kadaja M, Sumerina A, Verst T, Ojarand M, Ustav E, Ustav M. Genomic instability of the host cell induced by the human papillomavirus replication machinery. *EMBO J.* 2007;26(8):2180-2191. doi:10.1038/sj.emboj.7601665
- Adey A, Burton JN, Kitzman JO, et al. The haplotype-resolved genome and epigenome of the aneuploid HeLa cancer cell line. *Nature.* 2013;500(7461):207-211. doi:10.1038/nature12064
- Dall KL, Scarpini CG, Roberts I, et al. Characterization of naturally occurring HPV16 integration sites isolated from cervical keratinocytes under noncompetitive conditions. *Cancer Res.* 2008;68(20):8249-8259. doi:10.1158/0008-5472.CAN-08-1741
- Oyervides-Muñoz MA, Pérez-Maya AA, Rodríguez-Gutiérrez HF, et al. Understanding the HPV integration and its progression to cervical cancer. *Infect Genet Evol.* 2018;61:134-144. doi:10.1016/j.meegid.2018.03.003
- Martinez-Zapien D, Ruiz FX, Poirson J, et al. Structure of the E6/E6AP/p53 complex required for HPV-mediated degradation of p53. *Nature.* 2016;529(7587):541-545. doi:10.1038/nature16481
- Conrady MC, Suarez I, Gogl G, et al. Structure of high-risk papillomavirus 31 E6 oncogenic protein and characterization of E6/E6AP/p53 complex formation. *J Virol.* 2020;95(2):e00730-20. doi:10.1128/JVI.00730-20
- Rosenberger S, De-Castro Arce J, Langbein L, Steenbergen RD, Rosl F. Alternative splicing of human papillomavirus type-16 E6/E6* early mRNA is coupled to EGF signaling via Erk1/2 activation. *Proc*

- Natl Acad Sci USA*. 2010;107(15):7006-7011. doi:10.1073/pnas.1002620107
16. McNicol P, Guijon F, Wayne S, Hidajat R, Paraskevas M. Expression of human papillomavirus type 16 E6-E7 open reading frame varies quantitatively in biopsy tissue from different grades of cervical intraepithelial neoplasia. *J Clin Microbiol*. 1995;33(5):1169-1173. doi:10.1128/JCM.33.5.1169-1173.1995
 17. Olmedo-Nieva L, Munoz-Bello JO, Contreras-Paredes A, Lizano M. The role of E6 spliced isoforms (E6*) in human papillomavirus-induced carcinogenesis. *Viruses*. 2018;10(1):45. doi:10.3390/v10010045
 18. Guccione E, Pim D, Banks L. HPV-18 E6*1 modulates HPV-18 full-length E6 functions in a cell cycle dependent manner. *Int J Cancer*. 2004;110(6):928-933. doi:10.1002/ijc.20184
 19. Shally M, Alloul N, Jackman A, Muller M, Gissmann L, Sherman L. The E6 variant proteins E6I-E6IV of human papillomavirus 16: expression in cell free systems and bacteria and study of their interaction with p53. *Virus Res*. 1996;42(1-2):81-96. doi:10.1016/0168-1702(96)01301-9
 20. Pim D, Tomaic V, Banks L. The human papillomavirus (HPV) E6* proteins from high-risk, mucosal HPVs can direct degradation of cellular proteins in the absence of full-length E6 protein. *J Virol*. 2009;83(19):9863-9874. doi:10.1128/JVI.00539-09
 21. Cao C, Hong P, Huang X, et al. HPV-CCDC106 integration alters local chromosome architecture and hijacks an enhancer by three-dimensional genome structure remodeling in cervical cancer. *J Genet Genomics*. 2020;47(8):437-450. doi:10.1016/j.jgg.2020.05.006
 22. Cao C, Xu Q, Lin S, et al. Mapping long-range contacts between risk loci and target genes in human diseases with capture Hi-C. *Clin Transl Med*. 2020;10(5):e183. doi:10.1002/ctm2.183
 23. Ajiro M, Jia R, Zhang L, Liu X, Zheng ZM. Intron definition and a branch site adenosine at nt 385 control RNA splicing of HPV16 E6*1 and E7 expression. *PLoS One*. 2012;7(10):e46412. doi:10.1371/journal.pone.0046412
 24. Ning Y, Wang C, Liu X, et al. CK2-mediated CCDC106 phosphorylation is required for p53 degradation in cancer progression. *J Exp Clin Cancer Res*. 2019;38(1):131. doi:10.1186/s13046-019-1137-8
 25. Rusan M, Li YY, Hammerman PS. Genomic landscape of human papillomavirus-associated cancers. *Clin Cancer Res*. 2015;21(9):2009-2019. doi:10.1158/1078-0432.CCR-14-1101
 26. Ojesina AI, Lichtenstein L, Freeman SS, et al. Landscape of genomic alterations in cervical carcinomas. *Nature*. 2014;506(7488):371-375. doi:10.1038/nature12881
 27. Bodelon C, Untereiner ME, Machiela MJ, Vinokurova S, Wentzensen N. Genomic characterization of viral integration sites in HPV-related cancers. *Int J Cancer*. 2016;139(9):2001-2011. doi:10.1002/ijc.30243
 28. Nguyen ND, Deshpande V, Luebeck J, Mischel PS, Bafna V. ViFi: accurate detection of viral integration and mRNA fusion reveals indiscriminate and unregulated transcription in proximal genomic regions in cervical cancer. *Nucleic Acids Res*. 2018;46(7):3309-3325. doi:10.1093/nar/gky180
 29. Rosenberger S, De-Castro Arce J, Langbein L, Steenbergen RD, Rösl F. Alternative splicing of human papillomavirus type-16 E6/E6* early mRNA is coupled to EGF signaling via Erk1/2 activation. *Proc Natl Acad Sci USA*. 2010;107(15):7006-7011. doi:10.1073/pnas.1002620107
 30. Mesplède T, Gagnon D, Bergeron-Labrecque F, et al. p53 degradation activity, expression, and subcellular localization of E6 proteins from 29 human papillomavirus genotypes. *J Virol*. 2012;86(1):94-107. doi:10.1128/jvi.00751-11
 31. Brant AC, Menezes AN, Felix SP, de Almeida LM, Sammeth M, Moreira MAM. Characterization of HPV integration, viral gene expression and E6E7 alternative transcripts by RNA-seq: a descriptive study in invasive cervical cancer. *Genomics*. 2019;111(6):1853-1861. doi:10.1016/j.ygeno.2018.12.008
 32. Häfner N, Driesch C, Gajda M, et al. Integration of the HPV16 genome does not invariably result in high levels of viral oncogene transcripts. *Oncogene*. 2008;27(11):1610-1617. doi:10.1038/sj.onc.1210791
 33. Tang S, Tao M, McCoy JP Jr., Zheng ZM. The E7 oncoprotein is translated from spliced E6*1 transcripts in high-risk human papillomavirus type 16- or type 18-positive cervical cancer cell lines via translation reinitiation. *J Virol*. 2006;80(9):4249-4263. doi:10.1128/jvi.80.9.4249-4263.2006
 34. Scheffner M, Werness BA, Huibregtse JM, Levine AJ, Howley PM. The E6 oncoprotein encoded by human papillomavirus types 16 and 18 promotes the degradation of p53. *Cell*. 1990;63(6):1129-1136. doi:10.1016/0092-8674(90)90409-8
 35. Sedman SA, Barbosa MS, Vass WC, et al. The full-length E6 protein of human papillomavirus type 16 has transforming and trans-activating activities and cooperates with E7 to immortalize keratinocytes in culture. *J Virol*. 1991;65(9):4860-4866. doi:10.1128/jvi.65.9.4860-4866.1991
 36. Pim D, Banks L. HPV-18 E6*1 protein modulates the E6-directed degradation of p53 by binding to full-length HPV-18 E6. *Oncogene*. 1999;18(52):7403-7408. doi:10.1038/sj.onc.1203134
 37. Pim D, Massimi P, Banks L. Alternatively spliced HPV-18 E6* protein inhibits E6 mediated degradation of p53 and suppresses transformed cell growth. *Oncogene*. 1997;15(3):257-264. doi:10.1038/sj.onc.1201202
 38. Filippova M, Evans W, Aragon R, et al. The small splice variant of HPV16 E6, E6, reduces tumor formation in cervical carcinoma xenografts. *Virology*. 2014;450-451:153-164. doi:10.1016/j.virol.2013.12.011
 39. Vogelstein B, Lane D, Levine AJ. Surfing the p53 network. *Nature*. 2000;408(6810):307-310. doi:10.1038/35042675
 40. Cao X, Hou J, An Q, Assaraf YG, Wang X. Towards the overcoming of anticancer drug resistance mediated by p53 mutations. *Drug Resist Updat*. 2020;49:100671. doi:10.1016/j.drug.2019.100671
 41. Chao CC. Mechanisms of p53 degradation. *Clin Chim Acta*. 2015;438:139-147. doi:10.1016/j.cca.2014.08.015
 42. Hussain SP, Harris CC. p53 mutation spectrum and load: the generation of hypotheses linking the exposure of endogenous or exogenous carcinogens to human cancer. *Mutat Res*. 1999;428(1-2):23-32. doi:10.1016/s1383-5742(99)00028-9
 43. Zapatka M, Borozan I, Brewer DS, et al. The landscape of viral associations in human cancers. *Nat Genet*. 2020;52(3):320-330. doi:10.1038/s41588-019-0558-9
 44. Zhou J, Qiao X, Xiao L, et al. Identification and characterization of the novel protein CCDC106 that interacts with p53 and promotes its degradation. *FEBS Lett*. 2010;584(6):1085-1090. doi:10.1016/j.febslet.2010.02.031
 45. Han X, Zhou Z, Fei L, et al. Construction of a human cell landscape at single-cell level. *Nature*. 2020;581(7808):303-309. doi:10.1038/s41586-020-2157-4

SUPPORTING INFORMATION

Additional supporting information can be found online in the Supporting Information section at the end of this article.

How to cite this article: Zhi W, Wei Y, Lazare C, et al. HPV-CCDC106 integration promotes cervical cancer progression by facilitating the high expression of CCDC106 after HPV E6 splicing. *J Med Virol*. 2022;95:e28009. doi:10.1002/jmv.28009